Distinct mechanisms for activation of Cl^- and K^+ currents by Ca^{2+} from different sources in mouse sympathetic neurones

Juan Martínez-Pinna, Elspeth M. McLachlan* and Roberto Gallego

*Instituto de Neurociencias, Universidad Miguel Hernández-CSIC, Apartado 18, 03550 San Juan de Alicante, Spain and *Prince of Wales Medical Research Institute, Randwick, NSW 2031, Australia*

(Received 21 February 2000; accepted after revision 12 June 2000)

1. We have investigated the roles of different voltage-dependent Ca^{2+} channels in the activation of the Cl^- and K^+ channels responsible for the afterdepolarization (ADP) and slow afterhyperpolarization (AHP) in sympathetic neurones of the isolated mouse superior cervical ganglion *in vitro*.

2. The ADP and its associated Ca^{2+}-activated Cl^- current were markedly decreased by ω-agatoxin IVA (40–200 nM) and nifedipine (1–10 μM), but not by ω-conotoxin GVIA (300 nM).

3. In contrast, the AHP and the apamin-sensitive Ca^{2+}-activated K^+ current that underlies this potential were blocked by ω-conotoxin GVIA, but were not affected by ω-agatoxin IVA and were only slightly reduced by nifedipine.

4. Ryanodine (20 μM) reduced the Ca^{2+}-activated Cl^- current following an action potential by 75% but on average did not affect the Ca^{2+}-activated K^+ current.

5. Evidence that R-type channels provide a proportion of the Ca^{2+} activating both types of Ca^{2+}-dependent channel was obtained.

6. We conclude that Ca^{2+} entering through L- and P-type Ca^{2+} channels preferentially activates the Cl^- current responsible for the ADP in mouse sympathetic neurones, predominantly via Ca^{2+}-induced Ca^{2+} release, whereas the Ca^{2+} that activates the K^+ channels responsible for the AHP enters predominantly through N-type channels. The data can be explained by the selective association of each type of Ca^{2+} channel with particular intracellular mechanisms for activating other membrane channels, one indirect and the other direct, probably located at discrete sites on the soma and dendrites.

In mammalian sympathetic ganglion cells, Ca^{2+} entry during action potential firing activates K^+ and Cl^- conductances which contribute to slow afterpotentials (McAfee & Yarowsky, 1979; Sacchi *et al.* 1995; De Castro *et al.* 1997). In rat superior cervical ganglion (SCG) cells, which exhibit a long afterhyperpolarization (AHP), Ca^{2+} entry via N-type channels activates apamin-sensitive Ca^{2+}-activated K^+ channels (SK-type), which are responsible for most of the underlying conductance change (Davies *et al.* 1996). This conductance has been named $g_{K,Ca1}$ (Cassell & McLachlan, 1987*a*), to distinguish it from the slower Ca^{2+}-dependent conductance $g_{K,Ca2}$, which underlies a prolonged AHP in one subclass of sympathetic neurone, and from I_{AHP}, which differs in kinetic and pharmacological characteristics between several types of central neurone (Sah, 1996). On the other hand, in rat SCG cells, large conductance Ca^{2+}-activated K^+ channels (BK-type) are in part activated by Ca^{2+} entering through L-type channels, which has no effect on $g_{K,Ca1}$ (Davies *et al.* 1996). These observations suggest that Ca^{2+} entering through a specific channel type during the action potential (AP) is directed predominantly to a particular type of K^+ channel. Recently, N-type and BK-type channels in some cases, and L-type and SK-type channels in others, have been identified in single patches isolated from hippocampal somata, providing direct evidence for colocalization of pairs of functionally linked channels (Marrion & Tavalin, 1998). While the relative locations of Ca^{2+} and K^+ channels must be crucial in determining the electrical behaviour of neurones, these data imply that particular associations between channels are not necessarily the same for all neurone types. Data from sympathetic neurones have confirmed that, even for this one type of neurone, there are species differences and differences between phenotypically distinct classes of neurone in the way Ca^{2+} entry is linked to activation of BK and SK channels (Ireland *et al.* 1998; Davies *et al.* 1999).

In mouse SCG cells, Ca^{2+} entry during the AP activates, in addition to $g_{K,Ca1}$, a Cl^- conductance ($g_{Cl,Ca}$) that produces

an afterdepolarization (ADP; De Castro *et al.* 1997). When the cell is clamped at −55 mV, this is recorded as an inward current. About 45% of the high-voltage-activated Ca^{2+} current evoked by a step depolarization in dissociated mouse SCG somata flows through P/Q-type channels, 40% through N-type channels, 10% through L-type channels and a small proportion through channels resistant to known selective organic antagonists (here called R-type channels; Namkung *et al.* 1998). The question then arises as to how Ca^{2+} entering through these diverse types of voltage-dependent Ca^{2+} channel during an AP activates the Cl^- and K^+ conductances.

In this study, we have used pharmacological antagonists to distinguish the origin of the Ca^{2+} responsible for activation of Ca^{2+}-dependent afterpotentials in mouse sympathetic neurones. The experiments have utilized recordings from intact mouse SCG neurones, as the distribution of channels on the soma and dendrites is not uniform (e.g. Westenbroek *et al.* 1998) so that responses from dissociated somata will not necessarily reflect physiological events. Our data indicate that, as in rat SCG cells, the K^+ channels responsible for the slow AHP are activated mainly by Ca^{2+} entering through N-type channels, whereas Cl^- channel activation results from Ca^{2+} entering through L- and P-type Ca^{2+} channels. Ca^{2+}-induced Ca^{2+} release from intracellular stores is a major contributor to Cl^- channel activation but participates in K^+ channel activation in only a subgroup of cells. Some of the results have been presented in abstract form (Martínez-Pinna *et al.* 1998).

METHODS

The methods used for intracellular and voltage-clamp recording have been described previously (De Castro *et al.* 1997). Briefly, 5- to 7-week-old male mice (Swiss OF-1) were deeply anaesthetized by an I.P. injection of sodium pentobarbitone (40 mg kg^{-1}) and perfused through the heart with cold oxygenated saline. The superior cervical ganglion was taken from the animal and pinned to the Sylgard (Dow-Corning, Midland, MI, USA) bottom of a chamber continuously perfused with saline (mM: NaCl, 128; KCl, 5; $CaCl_2$, 2; NaH_2PO_4, 1; $NaHCO_3$, 16; $MgSO_4$, 1·2; and glucose, 5·5) equilibrated with 95% O_2–5% CO_2 (pH 7·4) at room temperature (22–25 °C). The ganglion was illuminated from one side by a fine fibre optic light source, allowing the cells on the surface to be seen using a microscope (×375–600). The experimental procedures were in accordance with the guidelines of the ethics committee of the Instituto de Neurociencias de la Universidad Miguel Hernández-CSIC.

Potentials were measured with respect to a Ag–AgCl pellet submerged in the outflow section of the bath. Cells were impaled with microelectrodes filled with 3 M KCl (50–90 MΩ) and data were collected only if the neurone generated APs of at least 70 mV in amplitude at the resting potential. The sampling frequency for discontinuous single-electrode current and voltage clamp was 2–6 kHz, with a duty cycle of 30/70 (Axoclamp 2B, Axon Instruments Inc.). Capacitance compensation was continuously monitored and adjusted to ensure head stage settling. Data were digitized and stored on a computer for subsequent analysis using commercial software (pCLAMP6, Axon Instruments Inc.). After impaling a cell, we waited for the membrane potential to stabilize and then measured the basic electrical properties at the resting membrane potential, including the amplitude and duration of the afterpotentials. Action potential half-width was measured as the duration at half the peak amplitude. Input resistance was calculated from the linear part of the *I–V* relationship determined near the end of 200 ms hyperpolarizing current pulses. APs were initiated after a 5 ms depolarizing current pulse or by a train, usually of six pulses at 40 Hz, and the ensuing afterpotentials were examined. To test the effect of the different drugs, we adjusted the membrane potential to −55 mV by passing current in discontinuous current-clamp mode before making measurements of APs and tail currents. Generally, we averaged five sweeps when a single AP was evoked and three when recording a train of discharges. To enable the degree of block to be quantified, cells were selected with relatively large outward tail currents (measures of $g_{K,Ca}$) or inward tail currents (measures of $g_{Cl,Ca}$) so that their responses are not necessarily representative of those of all SCG neurones.

Tail currents underlying the afterpotentials were measured using a hybrid clamp protocol in which APs were evoked with depolarizing current pulses and the amplifier was switched to voltage clamp mode, either after repolarization of a single AP, or 10 ms after the end of a brief train at 40 Hz. Tail currents were recorded under voltage clamp at −55 mV after filtering at 0·3 kHz and were analysed using commercial software (Origin, Microcal Software Inc., Northampton, MA, USA). After digital smoothing using a 9-point running average, the peak values were measured and the currents integrated from 20 ms after the peak of the AP in order to derive the amount of charge transferred. To test the effects of increasing Ca^{2+} loads on the current underlying the ADP, we could not use trains of > 10 APs because large ADPs were generated that reduced AP amplitude by inactivating Na^+ currents. Therefore, for these experiments, the cells were voltage clamped in the presence of 1 μM TTX and 100 nM apamin and trains of 5 ms pulses (to 0 mV from a holding potential of −55 mV) of varying duration at 40 Hz were applied. All values are expressed as means ± S.E.M. Statistical comparisons were made using Student's paired *t* test (Sigmastat, Jandel Scientific Software, Erkrath, Germany).

All drugs were obtained from Sigma, except nifedipine (RBI, Natick, MA, USA) and ω-agatoxin IVA (Peptides International, KY, USA), and were applied dissolved in the perfusing solution. Cytochrome *c* (0·1 mg ml^{-1}) was added to the toxin stock solutions to saturate non-specific peptide binding to the apparatus. Care was taken when using nifedipine to protect it from breakdown by light. The antagonists were used at concentrations that are relatively selective for different channel types. ω-Conotoxin GVIA blocks N-type channels quite selectively with an IC_{50} of 1–40 nM (Regan *et al.* 1991; Boland *et al.* 1994). ω-Agatoxin IVA blocks both P- and Q-type channels but with very different IC_{50} values of 1–20 nM and ~100 nM, respectively (Mintz *et al.* 1992; Randall & Tsien, 1995). Dihydropyridines block neuronal L-type channels with an IC_{50} of 0·3–2 μM (Jones & Jacobs, 1990; Regan *et al.* 1991). We usually applied a relatively high concentration of 10 μM, which is commonly used in intact neurones to ensure full blockade. This concentration has no non-specific actions in rat SCG cells (Davies *et al.* 1996). It should be noted, however, that 1 and 10 μM nifedipine had similar effects in the present experiments. Application of the drugs or toxins had significant effects on the input resistance, time constant, the holding current required to maintain the resting potential at −55 mV or the amplitude and duration of the AP only in the cases that are noted specifically.

RESULTS

Properties of SCG neurones of the mouse

The electrical properties of 71 mouse SCG neurones measured in control solution were: resting membrane potential, −51 ± 1·0 mV; AP amplitude, 99 ± 1·2 mV; AP half-width, 2·4 ± 0·1 ms; input resistance, 54 ± 3·1 MΩ; capacitance, 171 ± 10 pF; and time constant, 8·6 ± 0·6 ms.

Depolarizing and hyperpolarizing afterpotentials following AP firing varied greatly between neurones. In all cells, the fast AHP after repolarization of the AP was followed by a slow AHP (Fig. 1*B*). The slow AHP was separated from the fast AHP by a depolarizing inflection in 22% of the cells (Fig. 1*B*, arrow) including those cells (6%) in which the peak of this inflection was positive to the resting membrane potential, i.e. an ADP (Fig. 5*Aa*; see also De Castro *et al.* 1997). In all but six of the remaining cells, the transition from fast to slow AHP was marked by a change in the rate of depolarization (Fig. 2*Ba*, arrow). A train of six APs at 40 Hz generated an ADP followed by a slow AHP in 46% of cells (Fig. 1*C*; see also De Castro *et al.* 1997). In another 31% of cells, the membrane potential at the end of the train was more positive than the initial fast AHP (Fig. 3*Ab*), indicating that a depolarizing conductance had been activated during the train. In the remaining cells, the train generated a slow AHP that built up from the fast AHP. Thus, the relative magnitude of the conductances underlying the AHP and ADP differed between cells.

Afterpotentials depend on Ca^{2+} entry

As in other mammalian SCG cells (Adams & Harper, 1995), blockade of Ca^{2+} entry by addition of Cd^{2+} (100–500 μM) to the perfusate ($n = 9$) abolished both of the slower after-

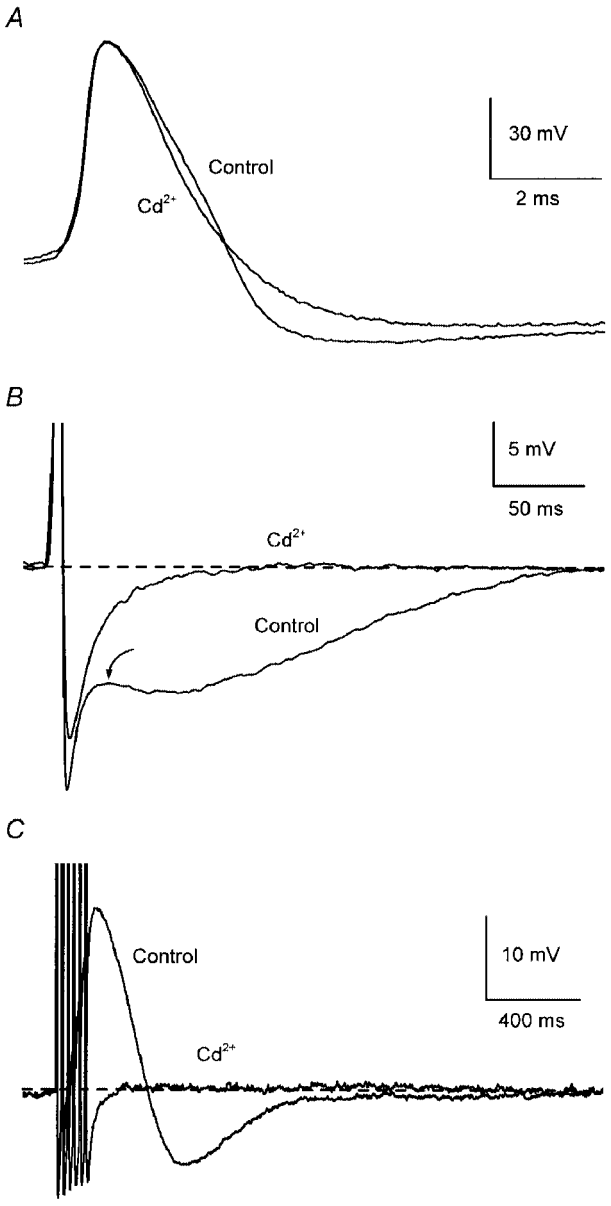

Figure 1. Ca^{2+}-dependent afterpotentials in mouse sympathetic ganglion cells

Records from a neurone in the superior cervical ganglion. *A*, addition of 500 μM Cd^{2+} reduced action potential (AP) half-width without affecting its amplitude. *B*, addition of Cd^{2+} abolished the depolarizing inflection following AP repolarization (arrow) and markedly reduced the afterhyperpolarization (AHP) following a single AP. *C*, addition of Cd^{2+} abolished the afterdepolarization (ADP) and reduced the AHP after a train of six APs at 40 Hz. APs in *B* and *C* are truncated (as in subsequent figures) and traces in control and test solutions have been superimposed with labels placed closest to the relevant trace. In these, and in the current-clamp records in subsequent figures, the dashed line indicates the baseline membrane potential, which was maintained close to −55 mV by passing current through the microelectrode.

Table 1. Effect of ωCgtx GVIA, ωAga IVA, nifedipine and ryanodine on $g_{Cl,Ca}$ in the presence of apamin

	Single action potential		Action potential train	
	Current peak (nA)	Total charge (pC)	Current peak (nA)	Total charge (pC)
Apamin ($n = 6$)	−0·08 ± 0·03	−6·7 ± 3·7	−1·7 ± 0·4	−279 ± 69
Apamin + ωCgtx GVIA	−0·09 ± 0·04	−8·6 ± 5·1	−1·5 ± 0·4	−255 ± 80
Apamin ($n = 10$)	−0·11 ± 0·01	−8·4 ± 0·9	−2·0 ± 0·3	−334 ± 58
Apamin + ωAga IVA	−0·06 ± 0·01**	−3·5 ± 0·9**	−1·2 ± 0·2**	−165 ± 36**
Apamin ($n = 9$)	−0·22 ± 0·06	−20·9 ± 7·6	−3·0 ± 0·6	−490 ± 119
Apamin + nifedipine	−0·09 ± 0·03**	−6·6 ± 2·6*	−1·5 ± 0·4**	−184 ± 53**
Apamin ($n = 5$)	−0·24 ± 0·05	−30·9 ± 7·9	−2·8 ± 0·9	−481 ± 158
Apamin + ryanodine	−0·09 ± 0·05*	−7·6 ± 4·4*	−2·2 ± 0·8*	−319 ± 131*

Tail currents after a single action potential or after a train of six action potentials at 40 Hz were recorded in voltage clamp at a holding potential of −55 mV. Inward Ca^{2+}-activated Cl^- currents were isolated by blocking $g_{K,Ca1}$ with 100 nM apamin. Changes after adding nifedipine (10 μM), ωCgtx GVIA (300 nM), ωAga IVA (40 nM) or ryanodine (20 μM) were compared using Student's paired t test (*$P < 0·05$; **$P < 0·01$).

Table 2. Effects of ωCgtx GVIA, ωAga IVA, nifedipine and ryanodine on $g_{K,Ca1}$ in the presence of 9AC

	Single action potential		Action potential train	
	Current peak (nA)	Total charge (pC)	Current peak (nA)	Total charge (pC)
9AC ($n = 5$)	0·32 ± 0·06	41·9 ± 12·4	0·72 ± 0·08	190 ± 31
9AC + ωCgtx GVIA	0·14 ± 0·03**	12·1 ± 4·2*	0·46 ± 0·08*	111 ± 31**
9AC ($n = 5$)	0·47 ± 0·06	75·5 ± 16·7	0·80 ± 0·08	329 ± 48
9AC + ωAga IVA	0·46 ± 0·05	74·0 ± 11·4	0·90 ± 0·08	371 ± 36
9AC ($n = 11$)	0·44 ± 0·03	62·2 ± 4·8	0·87 ± 0·05	290 ± 24
9AC + nifedipine	0·41 ± 0·03	50·0 ± 5·3*	0·94 ± 0·07	277 ± 21
9AC ($n = 7$)	0·39 ± 0·03	82·7 ± 17·7	0·66 ± 0·07	352 ± 64
9AC + ryanodine	0·33 ± 0·03	60·6 ± 8·0	0·63 ± 0·09	298 ± 47

Tail currents after a single action potential or after a train of six action potentials at 40 Hz were recorded in voltage clamp at a holding potential of −55 mV. Outward Ca^{2+}-activated K^+ currents were isolated by blocking $g_{Cl,Ca}$ with 2 mM 9AC. Changes after adding nifedipine (10 μM), ωCgtx GVIA (300 nM), ωAga IVA (40 nM) or ryanodine (20 μM) were compared using Student's paired t test (*$P < 0·05$; **$P < 0·01$).

potentials (when present) after a single AP (Fig. 1*B*) or a train of APs (Fig. 1*C*). Cd^{2+} also produced a 32% decrease in AP half-width (Fig. 1*A*; control, 2·2 ± 0·20 ms; Cd^{2+}, 1·5 ± 0·10 ms; $P < 0·01$).

Blockade of SK channels with apamin reveals $g_{Cl,Ca}$

As in the rat SCG (Kawai & Watanabe, 1986), apamin (100 nM) largely abolished the slow AHP (Fig. 2*A*). In 52% of 37 cells, addition of apamin to the control solution revealed an ADP after a single AP (Fig. 2*Aa*) and the same occurred after a train of APs in all but one cell, including those neurones in which only an AHP was detected in control solution. Apamin increased the amplitude and duration of ADPs after a train (Fig. 2*Ab*), generating repetitive discharges in 11 cells. In contrast, very rarely one or two APs occurred during a large ADP in control solution. These data indicate that, in most cells that lacked an ADP in control solution, activation of the Cl^- conductance after a single discharge was obscured by the K^+ conductance underlying the AHP.

When the cells were voltage clamped in control solution, the currents recorded at −55 mV after an AP had different shapes due to the variable amounts of inward Cl^- and outward K^+ conductances. There was usually an early inward inflection or plateau in the outward current after a single AP (Fig. 2*Ac* and *Bc*) but, after a train, a small net

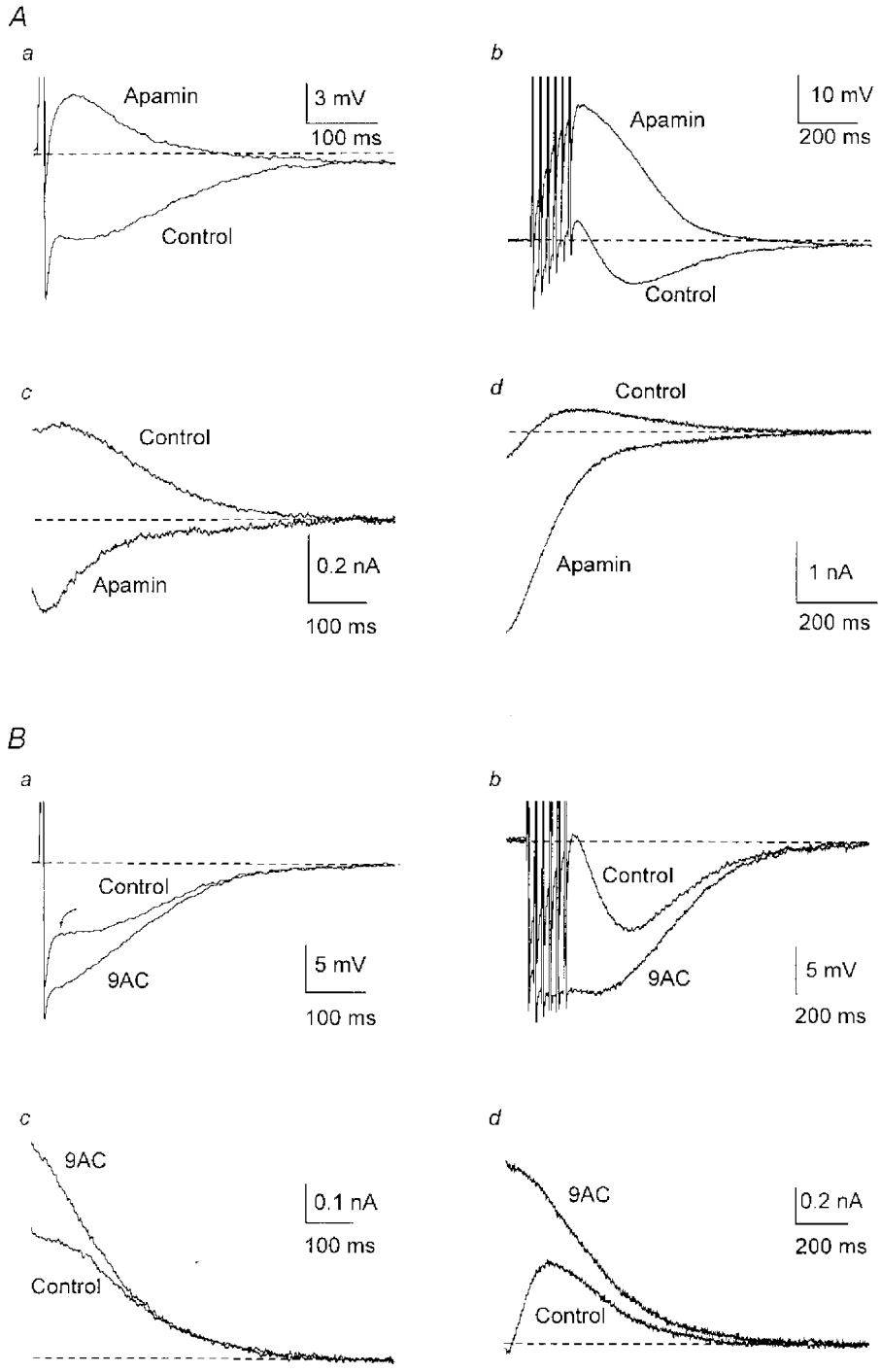

Figure 2. Apamin and 9AC reveal the Cl^- and K^+ currents underlying afterpotentials

Responses following a single AP are shown on the left (*a*) and after a train of six APs at 40 Hz on the right (*b*) in this and subsequent figures. *A*, in one cell, addition of apamin (100 nM in this and subsequent figures) abolished the slow AHP, revealing an ADP after one AP (*a*) and enhancing the ADP after a train of six APs at 40 Hz (*b*). In the same neurone, outward tail currents following a single AP (*c*) or a train of APs (*d*) were blocked by apamin, revealing inward tail currents. *B*, in another cell, addition of 9AC (2 mM in this and subsequent figures) reduced the depolarizing inflexion in the AHP after a single AP (*a*) and the small ADP following a train of APs (*b*), enhancing the AHP. Arrow points to the transition from fast to slow AHP. In the same neurone, 9AC blocked the inward currents after a single AP (*c*) and after a train of APs (*d*), enhancing the outward tail currents. In these, and in voltage-clamp records in the following figures, the dashed line indicates the holding current needed to keep the membrane potential at −55 mV. In this, and in the following figures except Fig. 5*Ab*, the trains consisted of six APs at 40 Hz.

inward current of variable amplitude was generated and was followed by an outward current (Fig. 2*Ad* and *Bd*). In the presence of apamin (100 nM), the outward tail currents were largely blocked, revealing a clear inward current after one AP (Fig. 2*Ac*) and increasing markedly the inward current that followed a train (Fig. 2*Ad*). The enhancement of the inward current after a train resulted in as much as 40 times the total charge transfer as that following a single AP (Table 1).

Thus application of 100 nM apamin reveals the inward Cl^- current, providing a measure of the Ca^{2+}-activated Cl^- conductance, $g_{Cl,Ca}$ (see Introduction). In all the voltage-clamp experiments on $g_{Cl,Ca}$ described below, 100 nM apamin was present throughout.

In 14 cells in which electrical properties were measured in control solution, apamin decreased the holding current needed to keep the resting membrane potential at −55 mV (from $-0{\cdot}43 \pm 0{\cdot}10$ to $-0{\cdot}29 \pm 0{\cdot}09$ nA, $P < 0{\cdot}05$) and also increased input resistance (from 43 ± 4 to 60 ± 8 MΩ, $P < 0{\cdot}05$). Apamin also increased AP amplitude (from 94 ± 2 to 101 ± 2 mV, $P < 0{\cdot}01$) but reduced AP duration (from $2{\cdot}6 \pm 0{\cdot}16$ to $2{\cdot}3 \pm 0{\cdot}13$ ms, $P < 0{\cdot}01$). These results suggest that apamin blocks a K^+ conductance that is active at −55 mV. Such a conductance was not detected in rat (Davies *et al.* 1996) or guinea-pig (Ireland *et al.* 1998) sympathetic neurones.

Blockade of Cl^- channels with 9AC reveals $g_{K,Ca1}$

As reported previously (De Castro *et al.* 1997), addition of the Cl^- channel blocker anthracene-9-carboxylic acid (9AC; 2 mM, $n = 21$) substantially reduced the amplitude of the ADP, increasing the amplitude and duration of the AHP (Fig. 2*Ba* and *b*) and the outward current carried by $g_{K,Ca1}$

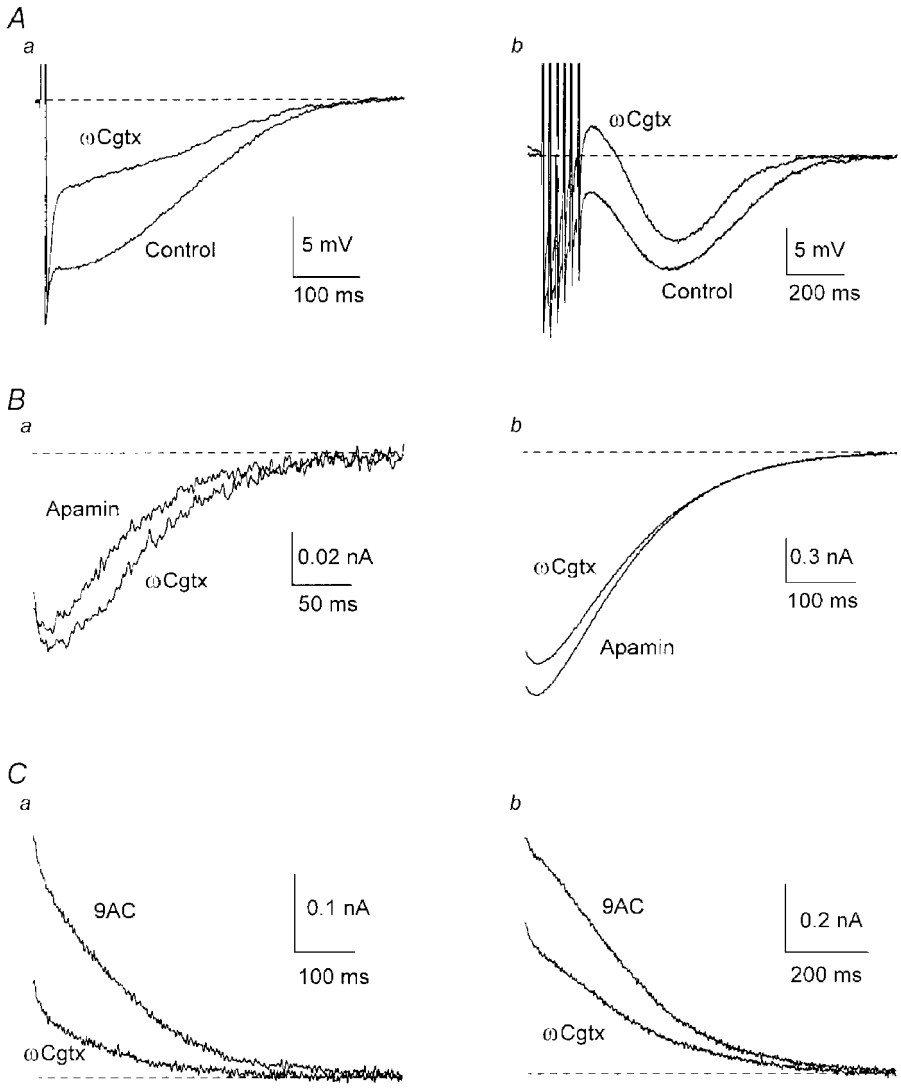

Figure 3. N-type Ca^{2+} channels contribute to activation of the AHP but not the ADP

A, in one cell, addition of 300 nM ω-Cgtx GVIA reduced the AHP, therefore increasing the ADP. *B*, averaged inward currents from six cells in the presence of apamin showed little variation when ω-Cgtx GVIA was added. *C*, averaged outward currents from five cells in the presence of 9AC were reduced when ω-Cgtx GVIA was added.

(Fig. 2*Bc* and *d*). In general, the degree of block produced by 9AC was more marked after a single AP than after a train. The enhancement of the outward current after the train resulted in about 4 times as much total charge transfer as that following a single AP (Table 2).

Thus, application of 2 mM 9AC reveals the outward K^+ current, providing a measure of the Ca^{2+}-activated K^+ conductance $g_{K,Ca1}$ (see Introduction). In all the voltage-clamp experiments on $g_{K,Ca1}$ described below, 2 mM 9AC was present throughout.

N-type Ca^{2+} channel block has no effect on $g_{Cl,Ca}$ but reduces $g_{K,Ca1}$

The N-type channel antagonist ω-conotoxin GVIA (ωCgtx GVIA, 300 nM) decreased the AHP in all cells tested ($n = 9$, Fig. 3*Aa*) and increased the ADP following a train of APs (Fig. 3*Ab*). On average, the membrane voltage measured at the end of the train shifted from $-2{\cdot}4 \pm 6{\cdot}1$ mV to $4{\cdot}2 \pm 5{\cdot}6$ mV ($P < 0{\cdot}001$). These results suggest that blockade of Ca^{2+} entry through N-type channels decreased activation of $g_{K,Ca1}$, as occurs in rat SCG neurones (Davies *et al.* 1996), allowing for a greater effect of $g_{Cl,Ca}$ in depolarizing the membrane following AP discharge.

N-type channels were not involved in the activation of $g_{Cl,Ca}$ because 300 nM ωCgtx GVIA had no significant effect on the mean inward current evoked after a single AP or a train of APs ($n = 6$; Fig. 3*B* and Table 1; see also Fig. 11*A*).

In contrast, ω-Cgtx GVIA reduced $g_{K,Ca1}$, the effect being larger on the outward tail current evoked by a single AP (Fig. 3*Ca*) than on that following a train (Fig. 3*Cb*), when measured as either charge transfer or mean peak outward current ($n = 5$; Table 2; see also Fig. 11*B*). Thus, Ca^{2+} entering through N-type channels activates $g_{K,Ca1}$.

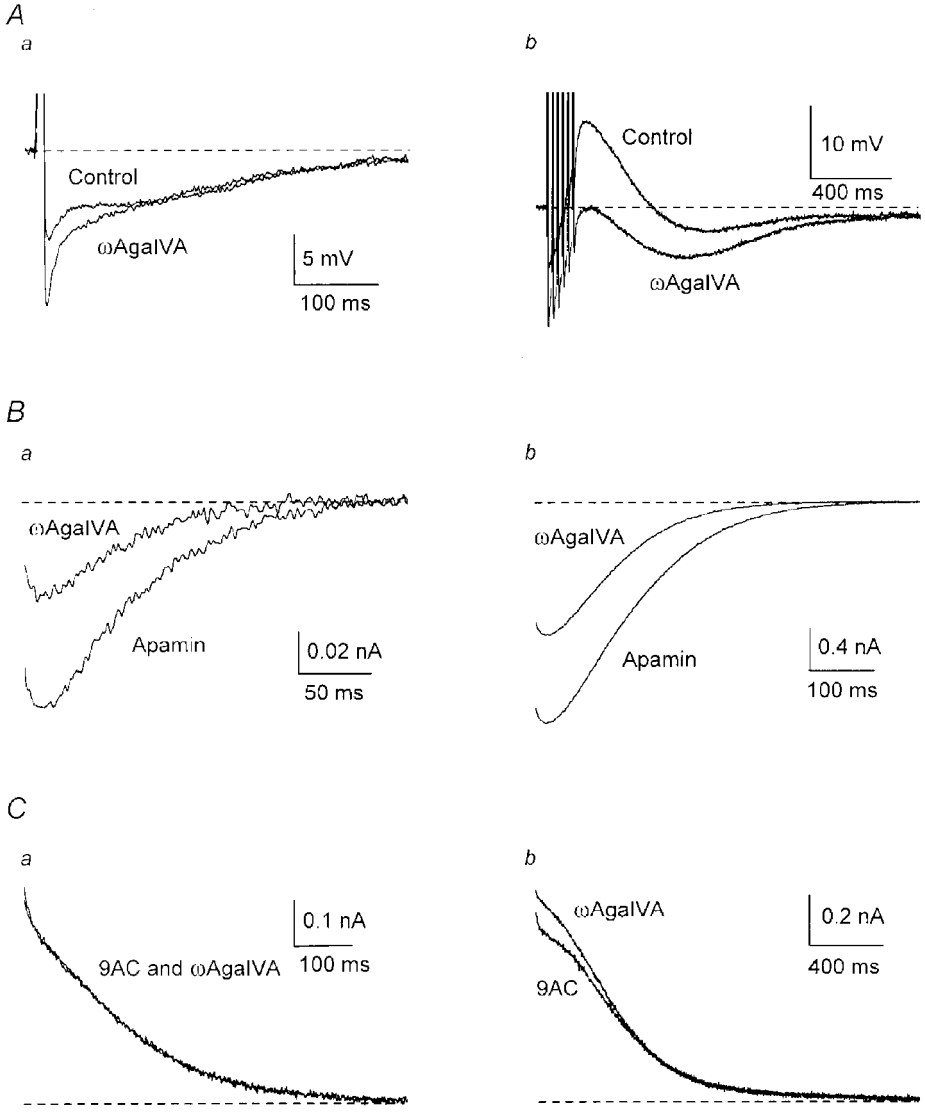

Figure 4. P-type Ca^{2+} channels contribute to activation of the ADP but not the AHP

A, in one cell, addition of ωAga IVA (40 nM) decreased the ADP, therefore increasing the AHP. *B*, averaged inward currents from 10 cells in the presence of apamin were partially blocked by ωAga IVA. *C*, averaged outward currents from five cells in the presence of 9AC showed little variation when ωAga IVA was added.

P-type Ca^{2+} channel block reduces $g_{Cl,Ca}$ but has no effect on $g_{K,Ca1}$

Relatively selective blockade of P-type channels can be achieved by using ω-agatoxin IVA (ωAga IVA) at concentrations < 50 nM, as the IC_{50} for Q-type channels is ~100 nM (Randall & Tsien, 1995). Application of ωAga IVA (40 nM, $n = 3$) always enhanced the AHP, particularly after a train of APs (Fig. 4*A*), suggesting that P-type channel block reduces the activation of $g_{Cl,Ca}$ without having much effect on $g_{K,Ca1}$.

In 10 cells, 40 nM ωAga IVA decreased peak inward current by 45% and charge transfer by about 60% after a single AP, the effect being slightly smaller after a train (Fig. 4*B* and Table 1; see also Fig. 11*A*). The peak inward current after a single AP was not affected by 20 nM ωAga IVA whereas peak current was reduced by 53% and charge transfer by 61% in 200 nM ωAga IVA ($n = 3$). This latter change was not significantly different from the effect of 40 nM ωAga IVA, suggesting that the toxin's action was more likely to have occurred by blockade of P-type than Q-type channels.

In contrast outward currents were not decreased by 40 nM ωAga IVA in any of the five cells studied (Fig. 4*C* and Table 2; see also Fig. 11*B*). These data indicate that Ca^{2+} entering through P-type channels has no effect on $g_{K,Ca1}$.

L-type Ca^{2+} channel block reduces $g_{Cl,Ca}$ but has little effect on $g_{K,Ca1}$

In 12 cells, the L-type Ca^{2+} channel antagonist nifedipine (10 μM) reduced or abolished the ADP that followed APs (Fig. 5*A*). In contrast, the peak amplitude of the slow AHP increased, consistent with the majority of the Ca^{2+} for

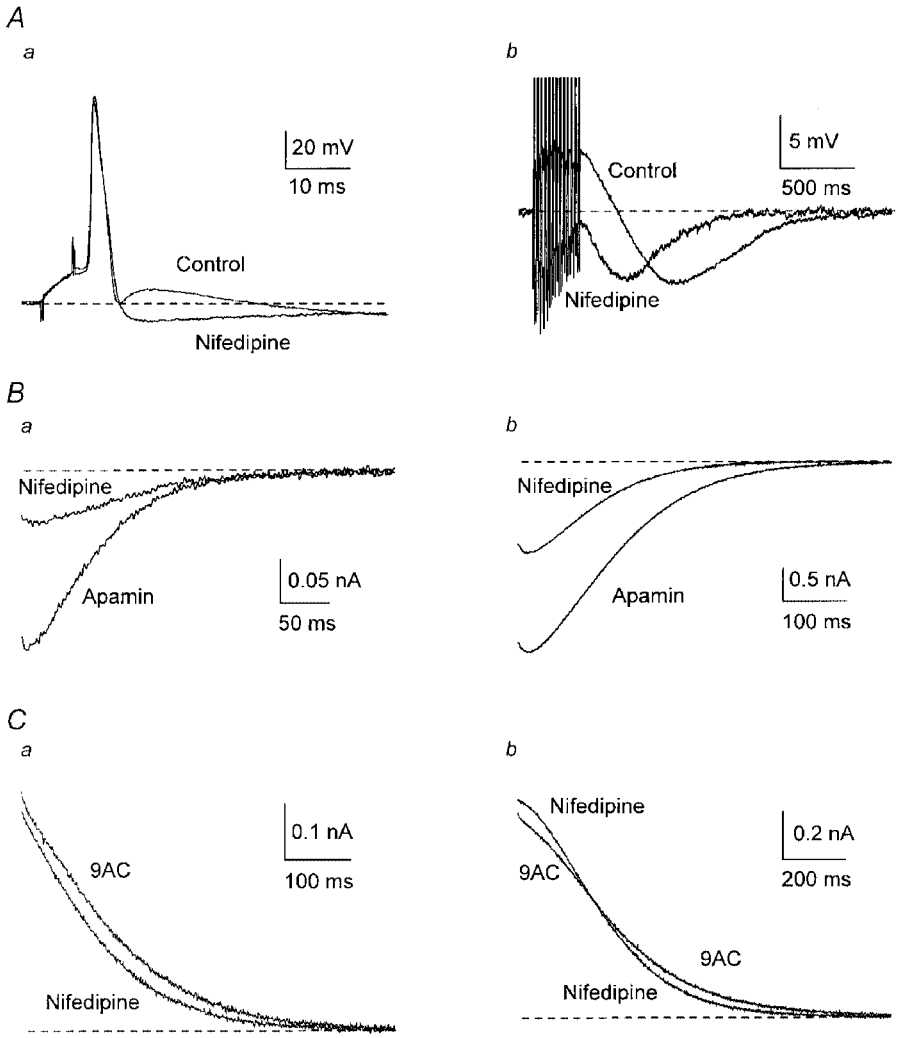

Figure 5. L-type Ca^{2+} channels contribute to activation of the ADP but have little effect on the AHP

A, addition of 10 μM nifedipine abolished the ADP revealing an AHP after one AP (*a*) and reduced the ADP without affecting AHP amplitude after a train of 13 APs (*b*). *B*, averaged inward currents from nine cells in apamin were reduced when nifedipine was added. *C*, averaged outward currents from 11 cells in the presence of 9AC showed, when nifedipine was added, a small decrease after a single AP (*a*) and a change in the time course after a train of APs (*b*).

activation of the slow AHP entering through channels other than L-type ones.

The amplitude and duration of $g_{Cl,Ca}$ were substantially reduced by 10 μM nifedipine ($n = 9$), both after a single AP and after a train (Fig. 5*B* and Table 1; see also Fig. 11*A*). These results suggest that, during an AP, the great majority of Ca^{2+} entering through L-type channels is directed towards activation of Cl^- channels with little effect on $g_{K,Ca1}$.

In agreement with this idea, nifedipine ($n = 11$) had no significant effect on the peak amplitude of the outward current after a single AP, although it produced a small significant reduction in charge transfer (Fig. 5*Ca* and Table 2; see also Fig. 11*B*). There was no significant effect after a train of APs (Table 2). However, the responses to nifedipine differed between cells, which could be separated into two distinct groups on the basis of the time course of decay of $g_{K,Ca1}$ (Fig. 6). In six of the 11 cells (type I), outward currents initially fell either above (Fig. 6*Aa*) or on the exponential fitted to the later decay of $g_{K,Ca1}$. In the remaining five cells (type II), there was a plateau during the early part of the outward current, so that the data fell below the extrapolated exponential (Fig. 6*Ba*; see also Fig. 8*Ca*). In type I cells, nifedipine had no significant effect on $g_{K,Ca1}$ after one AP and produced a small increase in the peak outward current after a train (from $0{\cdot}87 \pm 0{\cdot}09$ to $1{\cdot}00 \pm 0{\cdot}08$ nA, $P < 0{\cdot}05$). This increase could be due to concurrent block of residual $g_{Cl,Ca}$ (due to incomplete block by 9AC). In type II cells, nifedipine decreased $g_{K,Ca1}$ after one AP (Fig. 6*B*), blocking 35% of the charge transfer (from 69 ± 6 to 45 ± 10 pC, $P < 0{\cdot}05$) and 17% of the peak current (from $0{\cdot}42 \pm 0{\cdot}04$ to $0{\cdot}35 \pm 0{\cdot}06$ nA, $P < 0{\cdot}05$), but had no significant effect on $g_{K,Ca1}$ after a train. This suggests that, with low Ca^{2+} loads, such as those generated by a single AP, L-type channels are involved in the activation of $g_{K,Ca1}$ only in type II SCG neurones but not in type I neurones.

Ryanodine reduces $g_{Cl,Ca}$ but has little effect on $g_{K,Ca1}$

To investigate the contribution of Ca^{2+}-induced Ca^{2+} release (CICR) in the activation of $g_{Cl,Ca}$ and $g_{K,Ca1}$, we applied ryanodine (20 μM), which blocks Ca^{2+} release from intracellular stores (Meissner, 1994).

Ryanodine ($n = 5$) markedly decreased the inward current following an AP and to a lesser extent that following a train (Figs 7*A* and 11*A*, Table 1). This suggests that, after a single AP, $g_{Cl,Ca}$ is activated predominantly by CICR but, as

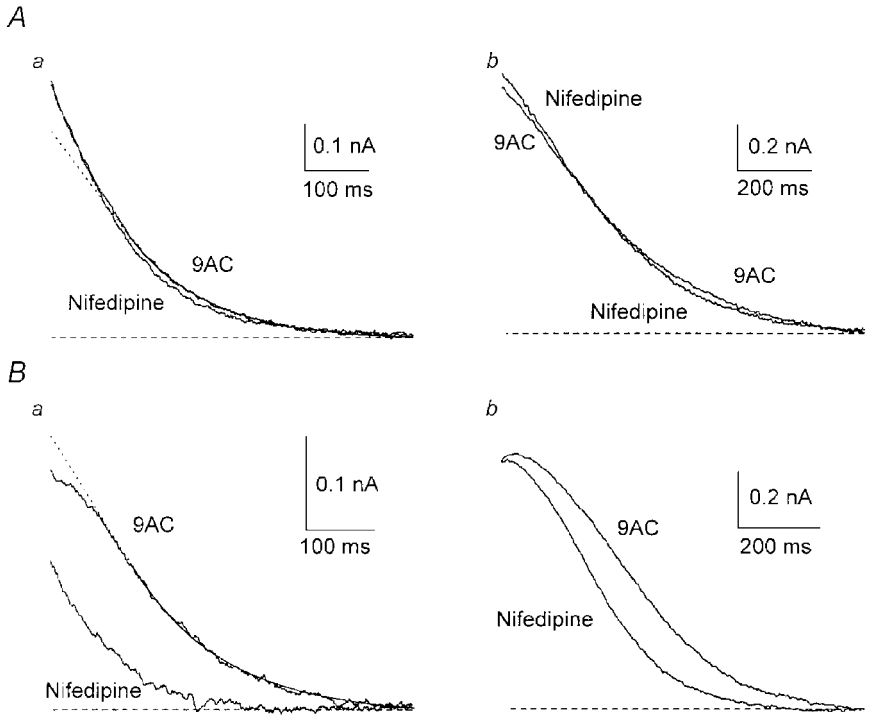

Figure 6. L-type Ca^{2+} channels contribute to activation of $g_{K,Ca1}$ in a subgroup of neurones

Two groups of cells were identified on the basis of the time course of the outward current recorded in the presence of 9AC. *A*, response of type I cells. When an exponential function was fitted to the outward current, starting 150 ms after the AP (continuous line), and extrapolated to the initial part (dotted line in this and subsequent figures), the outward current of type I cells either fitted the exponential well or initially fell above it (*a*). When 10 μM nifedipine was added, the outward current from a type I cell was not affected after one AP (*a*) and showed a small increase in peak current after a train (*b*). *B*, response of type II cells. The outward current of type II cells initially fell below the extrapolated exponential (*a*). In one type II cell, nifedipine markedly reduced $g_{K,Ca1}$ after one AP (*a*) and had a smaller effect on the latter part of the current after a train (*b*).

intracellular Ca^{2+} concentration increases, the proportion of Cl^- channels activated directly by Ca^{2+} entering the cell also increases. When the cells were challenged with pulse trains of increasing duration, the proportion of the peak inward current blocked by ryanodine decreased from about 75% for a single pulse to about 35% for the longer trains ($n = 5$; Fig. 7*B*). Thus, CICR plays an important role in activating $g_{Cl,Ca}$ when intracellular Ca^{2+} concentration is low (i.e. in the physiological range).

In contrast, ryanodine did not significantly affect the averaged outward currents ($n = 7$) recorded in 9AC (Fig. 8*A* and Table 2; see also Fig. 11*B*). However, if the above criteria were used to separate the cells on the basis of the decay of $g_{K,Ca1}$, the responses to ryanodine differed between type I and type II cells. In four type I cells, ryanodine had no significant effect (Fig. 8*B*) but in three type II cells (Fig. 8*C*) ryanodine clearly decreased the outward current after one AP (charge transfer, $46 \pm 1{\cdot}1$% block, $P < 0{\cdot}01$) and to a smaller degree after a train ($32 \pm 7{\cdot}0$% block, $P < 0{\cdot}05$). This suggests that CICR contributes to activation of $g_{K,Ca1}$ only in type II cells, in which it delays the decline in the outward current after an AP, whereas $g_{K,Ca1}$ is probably activated directly by Ca^{2+} entering through N-type channels in type I cells.

The effects of ryanodine on $g_{Cl,Ca}$ and on $g_{K,Ca1}$ in type II cells were almost identical to those of nifedipine. In other cell types, activation of CICR commonly occurs via the Ca^{2+} that enters through L-type channels (Shoshan-Barmatz & Ashley, 1998). We therefore tested the effects of adding ryanodine on the residual $g_{Cl,Ca}$ and $g_{K,Ca1}$ that remained after application of 10 μM nifedipine. In four cells, nifedipine blocked $g_{Cl,Ca}$ as described above, but subsequent application of ryanodine produced no significant change in $g_{Cl,Ca}$ (Fig. 9*A*). Similarly, nifedipine decreased $g_{K,Ca1}$ in four type II cells, but ryanodine did not reduce the current further (Fig. 9*B*). Thus, Ca^{2+} entry through L-type channels triggers the ryanodine-sensitive mechanism that activates $g_{Cl,Ca}$ and, in type II cells, $g_{K,Ca1}$.

Resistant Ca^{2+} channels contribute to both $g_{Cl,Ca}$ and $g_{K,Ca1}$

Because the degree of block of $g_{Cl,Ca}$ was similar (about 65%) when either P- or L-type channels were blocked, we examined whether R-type channels were involved in the activation of $g_{Cl,Ca}$ by applying both ωAga IVA (40–200 nM) and nifedipine (1–10 μM) in the presence of 100 nM apamin ($n = 4$). After a single AP, charge transfer was blocked by about 70% and peak current by about 65%, whereas after a train, block was about 70 and 60%, respectively (Figs 10*A*

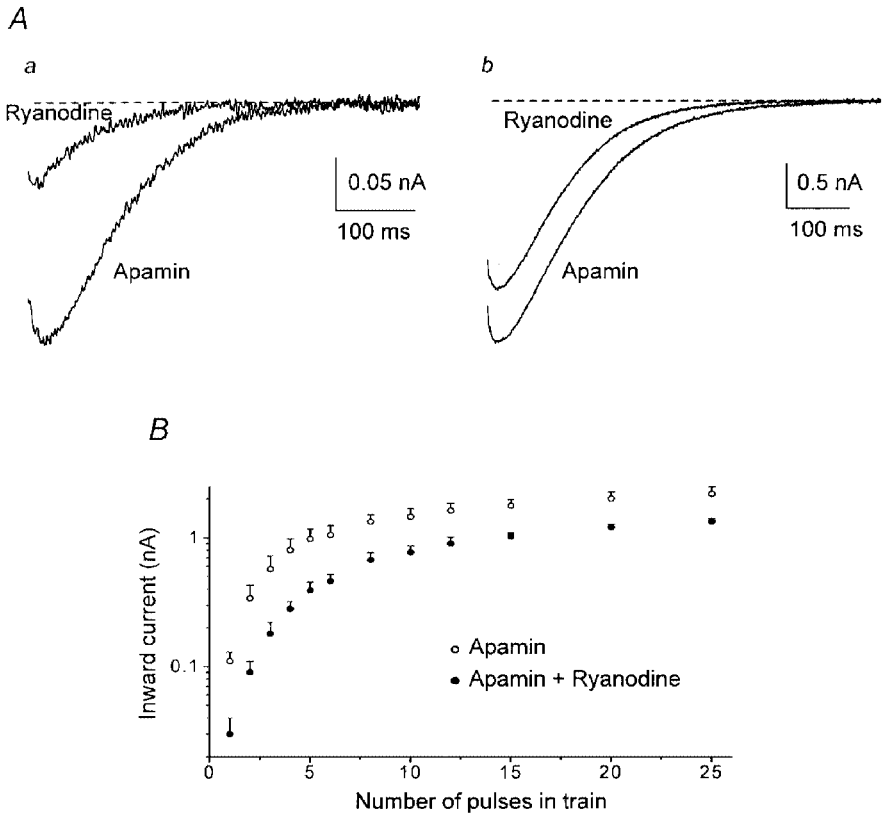

Figure 7. Ca^{2+}-induced Ca^{2+} release contributes to activation of $g_{Cl,Ca}$

A, averaged inward currents from five cells in the presence of apamin were markedly reduced after one AP when 20 μM ryanodine was added (*a*) but less so after a train (*b*). *B*, mean inward currents from five cells following 5 ms depolarizing pulses (to 0 mV from −55 mV) applied at 40 Hz, plotted against the number of pulses in the train. The reduction in peak current was larger (75%) when one or two pulses were applied than when the train was prolonged (35%). Note the logarithmic ordinate. Error bars show S.E.M.

and 11*A*). Given the lack of effect of N-type channel blockers on $g_{Cl,Ca}$, this result indicates that R-type channels contributed to activation of the inward current.

To test whether Ca^{2+} entering through R-type channels also activates $g_{K,Ca1}$, we applied nifedipine (10 μM) and ωCgtx GVIA (300 nM) in the presence of 2 mM 9AC ($n = 3$). Overall block of the outward current was much greater after a single AP (charge transfer about 85%, peak current about 75%) than after a train (charge transfer about 50%, peak current 30%; Figs 10*B* and 11*B*), but there was clearly a fraction of $g_{K,Ca1}$ resistant to both drugs, even after a single AP, because 300 μM Cd^{2+} blocked the remaining current. Since P-type channel block did not affect $g_{K,Ca1}$, this result suggests that Ca^{2+} entry through R-type channels contributes to activation of $g_{K,Ca1}$.

DISCUSSION

Our main conclusion is that activation of the Cl^- conductance ($g_{Cl,Ca}$) responsible for the ADP following APs in mouse SCG neurones involves Ca^{2+} entering through P- and L-type channels and acting via Ca^{2+} release from ryanodine-sensitive intracellular stores. In contrast, the K^+ conductance responsible for the slow AHP ($g_{K,Ca1}$) is activated predominantly by Ca^{2+} entering through N-type channels. Assuming that our pharmacological tools provide selective and complete blockade, we can conclude that a smaller proportion of both currents is activated directly by Ca^{2+} entering through R-type channels.

These conclusions rest on the assumption that nifedipine, ωCgtx GVIA and ωAga IVA did not directly block Cl^- or K^+ channels. None of these drugs had effects on AP amplitude or passive properties, indicating that they do not

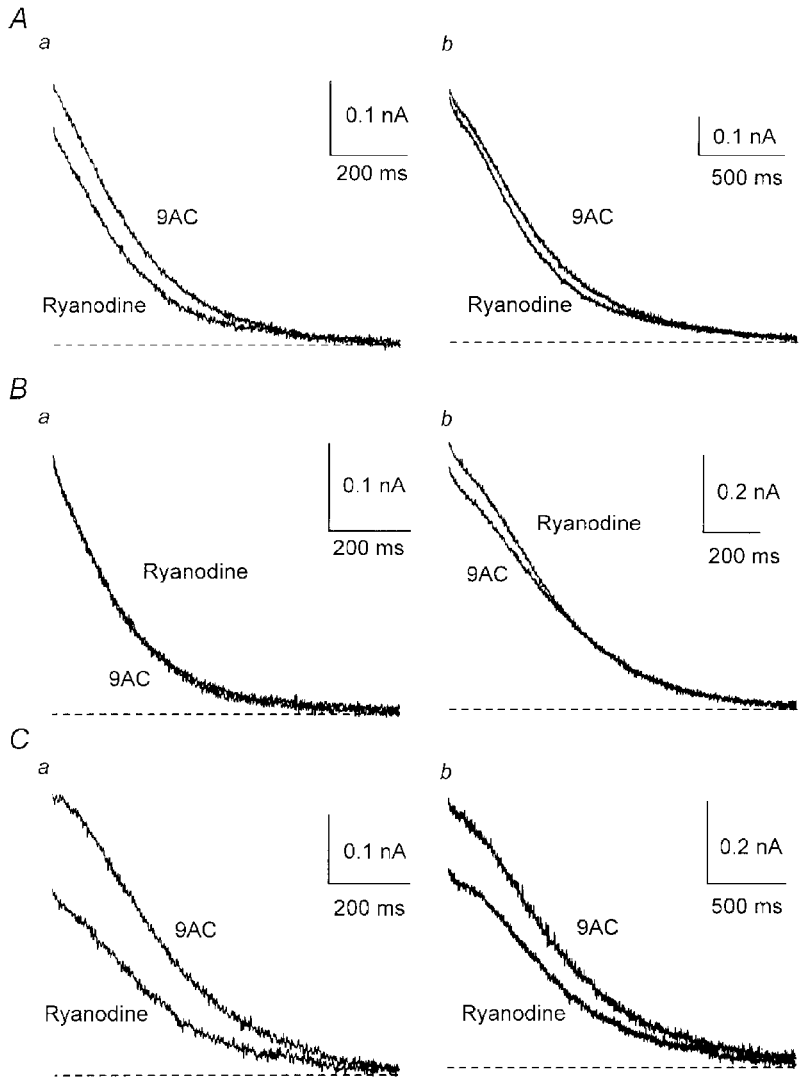

Figure 8. Ca^{2+}-induced Ca^{2+} release contributes to activation of $g_{K,Ca1}$ only in type II cells

A, ryanodine (20 μM), applied after 9AC, had no significant effect on the averaged outward currents from seven cells. When the cells were separated into two groups as in Fig. 6, ryanodine did not significantly affect the averaged outward currents from four type I cells (*B*) but decreased $g_{K,Ca1}$ in three type II cells (*C*) after a single AP (*a*) and after a train (*b*).

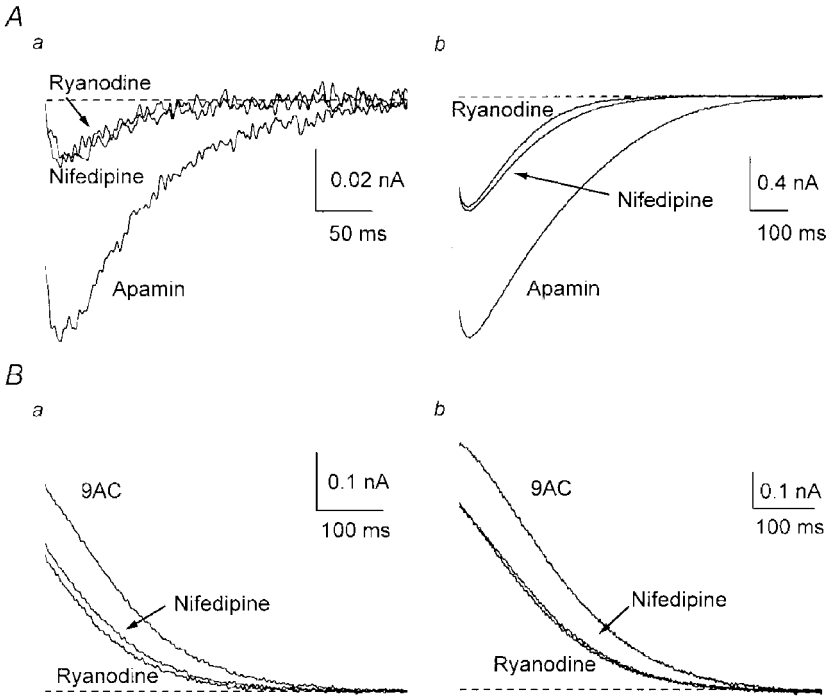

Figure 9. Ca^{2+}-induced Ca^{2+} release is activated by Ca^{2+} entering through L-type channels
A, averaged inward tail currents from four cells in the presence of apamin were decreased by 10 μM nifedipine, but showed no significant reduction when 20 μM ryanodine was added. *B*, averaged outward tail currents from four type II cells were decreased by nifedipine, but not by subsequent addition of ryanodine.

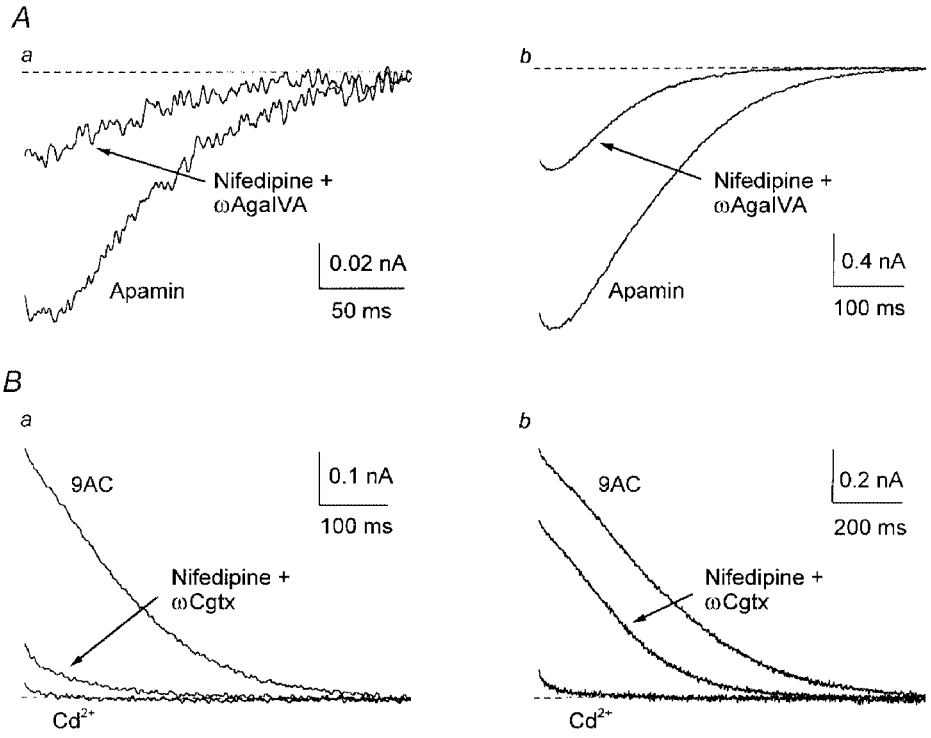

Figure 10. R-type channels contribute to activation of the currents underlying afterpotentials
A, averaged inward tail currents from four cells in the presence of apamin were markedly reduced, but not completely abolished, in the presence of 40 nM ωAga IVA and 10 μM nifedipine. *B*, averaged outward tail currents from three cells in the presence of 9AC were markedly reduced, but not completely blocked, in the presence of 10 μM nifedipine and 300 nM ωCgtx GVIA. Subsequent addition of 300 μM Cd^{2+} blocked the remaining outward currents.

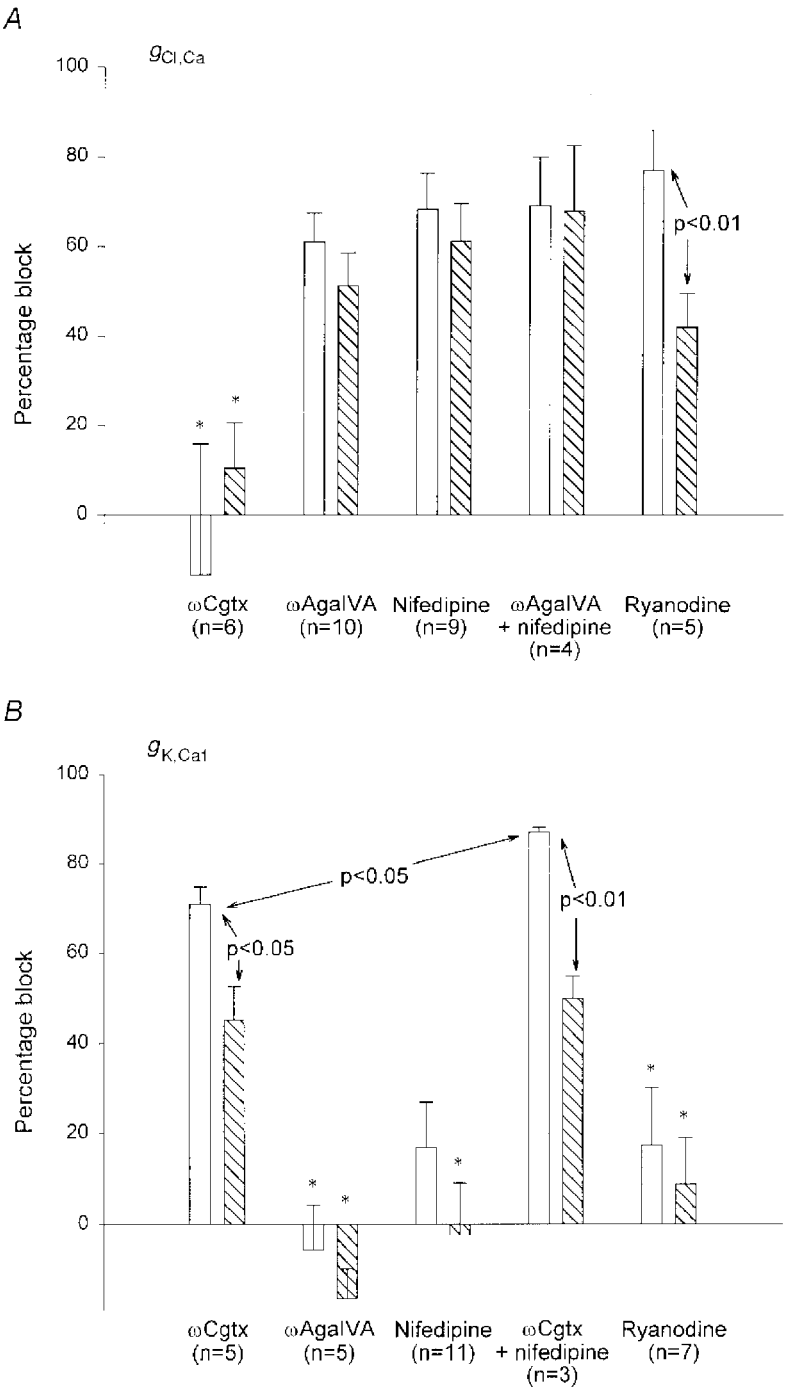

Figure 11. Percentage block of Ca^{2+}-activated Cl^- and K^+ conductances following different treatments suggests the mechanisms of their activation by APs

Changes in $g_{Cl,Ca}$ (*A*) and changes in $g_{K,Ca1}$ (*B*) (measured as total charge transfer) produced by ωCgtx GVIA, ωAga IVA, nifedipine and ryanodine (see also Tables 1 and 2). □, effect after a single AP; ▨, effect following a train. Data were obtained in the presence of 100 nM apamin (*A*) or 2 mM 9AC (*B*). Error bars indicate S.E.M. Statistically significant comparisons between different groups are indicated. All changes were significantly different from control (in the absence of any Ca^{2+} current blocker) except those marked * (see Tables 1 and 2). $g_{Cl,Ca}$ was blocked to a similar extent by all treatments except ωCgtx GVIA. The data suggest that Ca^{2+} from P- and L-type channels must act together to release Ca^{2+} from intracellular stores that, in turn, activates Cl^- channels underlying the ADP. In contrast, ωCgtx GVIA markedly reduced $g_{K,Ca1}$, suggesting a direct link between Ca^{2+} entering through N-type channels and SK channels underlying the AHP. A small amount of Ca^{2+} entry through L-type channels also contributes to activation of SK channels in type II cells. See text for further discussion.

interfere with Na^+ currents or most K^+ currents as previously shown in rat SCG neurones (Davies *et al.* 1996). This is in agreement with the known specificity of ωCgtx GVIA for N-type Ca^{2+} channels (Olivera *et al.* 1994) and of ωAga IVA for P/Q-type channels (Randall & Tsien, 1995). Also, ryanodine did not directly affect Ca^{2+}, K^+ or Cl^- channels because AP shape and input resistance were not modified. Furthermore, the currents generated by $g_{K,Ca1}$ in type I cells were not reduced in the presence of ryanodine.

Activation of $g_{Cl,Ca}$

Our results after blocking $g_{K,Ca1}$ with apamin demonstrate that most, if not all, normal mouse SCG neurones express $g_{Cl,Ca}$, as suggested by De Castro *et al.* (1997). Also, when 9AC was applied to cells that apparently lacked an ADP, the AHP became larger, indicating that blockade of $g_{Cl,Ca}$ allowed $g_{K,Ca1}$ to hyperpolarize the membrane further.

The function of $g_{Cl,Ca}$ in sympathetic neurones is not clear (e.g. Sánchez-Vives & Gallego, 1994). When SK channels were blocked with apamin, the ADP often generated APs, which is very rare in control solution (Sánchez-Vives & Gallego, 1994; De Castro *et al.* 1997). This suggests that decreases in the AHP, either indirectly following inhibition of N-type channels by e.g. catecholamines and neuropeptides (Toth & Miller, 1995), or directly following inhibition of SK-type channels by e.g. muscarinic agonists (Cassell & McLachlan, 1987*b*), might lead to repetitive discharge. Thus the Cl^- conductance underlying the ADP is expressed to a greater or lesser extent in all mouse SCG neurones where it could play a role in generating bursts of activity. However, this mechanism to increase firing appears to be absent from normal sympathetic neurones of other species (Cassell & McLachlan, 1987*a*; Sánchez-Vives & Gallego, 1994).

Activation of $g_{Cl,Ca}$ was dependent on Ca^{2+} entering through L-, P- and R-type channels (Fig. 11*A*). Functional coupling between L-type channels and Cl^- channels in sensory neurones has been previously implied by the potentiation of Cl^- tail currents by BayK8644, an L-type channel agonist (Scott *et al.* 1988). Although L- and N-type channels have been implicated in the activation of Ca^{2+}-dependent Cl^- currents in rabbit parasympathetic neurones (Akasu *et al.* 1990), ωCgtx GVIA did not affect $g_{Cl,Ca}$ in mouse SCG neurones.

After one AP, $g_{Cl,Ca}$ was blocked by about 70% by ryanodine (Fig. 11*A*), indicating that CICR plays an important role in its activation. The fact that either L- or P-type channel blockade reduced $g_{Cl,Ca}$ by approximately the same amount (Fig. 11*A*) suggests that Ca^{2+} entering through these channels activates CICR. The lack of effect of ryanodine on $g_{Cl,Ca}$ and $g_{K,Ca1}$ when applied after nifedipine confirms this for L-type channels, as has been shown in muscle cells (Shoshan-Barmatz & Ashley, 1998) and some neurones (Osmanovic & Shefner, 1993; Tanabe *et al.* 1998; Cordoba-Rodriguez *et al.* 1999). It appears, however, that both L- and P-type channels are needed simultaneously to trigger CICR in mouse SCG neurones, because a similar degree of block (70%) was produced when the two drugs were applied together (Fig. 11*A*). As the amounts of Ca^{2+} entering through each type of channel during an AP are quite different (J. Martínez-Pinna & R. Gallego, unpublished observations), they presumably act co-operatively but non-linearly in activating CICR. As the amount of $g_{Cl,Ca}$ (30%) remaining after combined blockade of L- and P-type channels (Fig. 11*A*) was similar to the ryanodine-insensitive component, Ca^{2+} entry through R-type channels probably activates $g_{Cl,Ca}$ directly.

The fact that the degree of block of $g_{Cl,Ca}$ by nifedipine and ωAga IVA was similar after a single AP and after a train of six APs (when the peak inward current was about 16 times larger) implies that 'spill over' from channels other than L- and P-type was relatively ineffective in activating $g_{Cl,Ca}$. This suggests that CICR activation of $g_{Cl,Ca}$ is spatially restricted (Berridge, 1998). This arrangement would allow CICR to deliver the concentration of Ca^{2+} necessary for activation of $g_{Cl,Ca}$ because the Ca^{2+} sensitivity of the Cl^- channels is relatively low (EC_{50} ~25 μM; Gomez-Hernandez *et al.* 1997; Hallani *et al.* 1998). In contrast, after a train of six APs, ryanodine produced a smaller degree of block (40%, Fig. 11*A*) than that produced by nifedipine and ωAga IVA (65%), suggesting that Ca^{2+} entering through L- and P-type channels, as well as through R-type channels, can activate $g_{Cl,Ca}$ directly when the neurone is overloaded with Ca^{2+} (see Fig. 7). Since sympathetic ganglion cells fire *in vivo* at low frequencies (McLachlan *et al.* 1997), the physiological activation of $g_{Cl,Ca}$ probably depends primarily on CICR mechanisms. Recent evidence in dorsal root ganglion neurones confirms that Cl^- channels can be activated by Ca^{2+} released from intracellular stores during one AP (Ayar & Scott, 1999).

Activation of $g_{K,Ca1}$

Activation of $g_{K,Ca1}$ after a single AP is clearly dependent on Ca^{2+} entry through N-type channels (Fig. 11*B*). This dependence is in agreement with findings in rat hypoglossal (Viana *et al.* 1993), vagal (Sah, 1995), sympathetic (Davies *et al.* 1996) and trigeminal (Kobayashi *et al.* 1997) neurones and guinea-pig sympathetic neurones (Ireland *et al.* 1998), as well as lamprey spinal neurones (Wikström & El Manira, 1998). Because $g_{K,Ca1}$ primarily involves SK channels, the functional link between these and N-type Ca^{2+} channels is therefore common to many neurones (cf. Marrion & Tavalin, 1998). On the other hand, R-type channels also contribute to $g_{K,Ca1}$ activation because the combined application of nifedipine and ωCgtx GVIA did not abolish the outward current (Fig. 11*B*).

Ryanodine had different effects in two subtypes of mouse SCG neurone that could be separated on the basis of the time course of $g_{K,Ca1}$. In type II cells, in which $g_{K,Ca1}$ showed a plateau before it declined, CICR activated about half of the current after one AP, whereas in type I cells in which $g_{K,Ca1}$ declined exponentially, CICR played no significant role. A small contribution of CICR (30%) to

$g_{K,Ca1}$ was previously reported in guinea-pig prevertebral sympathetic neurones (Jobling *et al.* 1993). Because nifedipine inhibited $g_{K,Ca1}$ and blocked the effect of ryanodine only in type II cells, its action is most likely to have been to prevent activation of CICR. According to this interpretation, $g_{K,Ca1}$ activation in type I neurones depends entirely on Ca^{2+} entering through N- and R-type channels, whereas in type II neurones, Ca^{2+} release induced by Ca^{2+} entering through L-type channels is also involved. L-type channels, CICR and Ca^{2+}-activated K^+ (SK) channels are functionally linked in vascular smooth muscle (Jaggar *et al.* 1998) and hippocampal neurones (Tanabe *et al.* 1998).

The contribution of R-type channels to $g_{K,Ca1}$ activation was substantially larger after a train than after one AP (Fig. 11*B*), consistent with 'spill over' of accumulated Ca^{2+}. Under these conditions, there was only slight inhibition of $g_{K,Ca1}$ by nifedipine or ryanodine in type II cells (Figs 6*Bb* and 8*Cb*), consistent with the saturation of CICR by Ca^{2+} influx after a few APs.

Distinct intracellular mechanisms for activation of Cl^- and K^+ channels

The physical bases for the functional links between Ca^{2+} and K^+/Cl^- channels in intact neurones are not known. The present results could be explained if, in mouse SCG neurones, L- and P-type channels are linked to an intracellular pathway, perhaps the store in the subsurface cisternae (Berridge, 1998), from which Ca^{2+} release directly activates membrane Cl^- channels, whereas N-type channels are closely juxtaposed to SK channels. R-type channels provide Ca^{2+} that activates both Cl^- and SK channels, to a much greater extent following a train of APs, and so they may be more widely distributed. Colocalization of Ca^{2+} and K^+ channels has been demonstrated directly at the neuromuscular junction, where BK channels are located adjacent to N-type channels in the presynaptic terminal (Robitaille *et al.* 1993), and in membrane patches from hippocampal somata (Marrion & Tavalin, 1998). In the latter case, N-type, SK and BK channels were present in the same somatic patch but SK channels were not activated by Ca^{2+} entering through the N-type channels, suggesting that some form of direct linkage between channels can exist at the molecular level.

Another possibility is that the different channels are located in separate regions of the cell (Davies *et al.* 1996). Although a dendritic location for high-threshold Ca^{2+} channels in sympathetic neurones has been proposed (Hirst & McLachlan, 1986), no data are available about the distribution of the different channel types in the somatodendritic membrane. In central neurones, L-type channels, although present in distal dendrites, are more common in the cell body and proximal dendrites, whereas N-type channels are more or less equally expressed in both cellular compartments (Westenbroek *et al.* 1998). Based on indirect evidence, it has been proposed that the Cl^- channels responsible for the ADP are located in the dendrites (Sánchez-Vives & Gallego, 1994; De Castro *et al.* 1997) which, in mouse SCG neurones, are relatively few in number and short. If this were the case, L- and P-type Ca^{2+} channels may also be located on the dendrites. There might even be two distinct populations of Cl^- channels in mouse SCG cells: a larger one that is activated via intracellular pathways dependent on Ca^{2+} entering via L- and P-type channels and another population that is activated by Ca^{2+} derived from R-type channels. While the second population of Cl^- channels might be activated either directly or indirectly, it is likely to be spatially distinct from the Cl^- channels dependent on Ca^{2+} entering via L- and P-type channels.

In conclusion, our results provide the first evidence for distinct mechanisms linking the physiological entry of Ca^{2+} through particular channel types during AP firing with the activation of Cl^- and K^+ membrane conductances in the same neurone. The data confirm that general intracellular Ca^{2+} levels are unlikely to reflect the localized consequences of Ca^{2+} influx through specific channels during physiological events.

Adams, D. J. & Harper, A. A. (1995). Electrophysiological properties of autonomic ganglion neurons. In *Autonomic Ganglia*, ed. McLachlan, E. M., pp. 153–212. Harwood Academic Publishers, Luxembourg.

Akasu, T., Nishimura, T. & Tokimasa, T. (1990). Calcium-dependent chloride current in neurones of the rabbit pelvic parasympathetic ganglia. *Journal of Physiology* **422**, 303–320.

Ayar, A. & Scott, R. H. (1999). The actions of ryanodine on Ca^{2+}-activated conductances in rat cultured DRG neurones; evidence for Ca^{2+}-induced Ca^{2+} release. *Naunyn-Schmiedeberg's Archives of Pharmacology* **359**, 81–91.

Berridge, M. J. (1998). Neuronal calcium signalling. *Neuron* **21**, 13–26.

Boland, L. M., Morrill, J. A. & Bean, B. P. (1994). ω-Conotoxin block of N-type calcium channels in frog and rat sympathetic neurons. *Journal of Neuroscience* **14**, 5011–5027.

Cassell, J. F. & McLachlan, E. M. (1987*a*). Two calcium-activated potassium conductances in a subpopulation of coeliac neurones of guinea-pig and rabbit. *Journal of Physiology* **394**, 331–349.

Cassell, J. F. & McLachlan, E. M. (1987*b*). Muscarinic agonists block five different potassium conductances in guinea-pig sympathetic neurones. *British Journal of Pharmacology* **91**, 259–261.

Cordoba-Rodriguez, R., Moore, K. A., Kao, J. P. Y. & Weinreich, D. (1999). Calcium regulation of a slow post-spike hyperpolarization in vagal afferent neurons. *Proceedings of the National Academy of Sciences of the USA* **96**, 7650–7657.

Davies, P. J., Ireland, D. R. & McLachlan, E. M. (1996). Sources of Ca^{2+} for different Ca^{2+}-activated K^+ conductances in neurones of the rat superior cervical ganglion. *Journal of Physiology* **495**, 353–366.

Davies, P. J., Ireland, D. R., Martínez-Pinna, J. & McLachlan, E. M. (1999). Electrophysiological roles of L-type channels in different classes of guinea pig sympathetic neuron. *Journal of Neurophysiology* **82**, 818–828.

De Castro, F., Geijo-Barrientos, E. & Gallego, R. (1997). Calcium-activated chloride current in normal mouse sympathetic ganglion cells. *Journal of Physiology* **498**, 397–408.

Gomez-Hernandez, J. M., Stühmer, W. & Parekh, A. B. (1997). Calcium dependence and distribution of calcium-activated chloride channels in *Xenopus* oocytes. *Journal of Physiology* **502**, 569–574.

Hallani, M., Lynch, J. W. & Barry, P. H. (1998). Characterization of calcium-activated chloride channels in patches excised from the dendritic knob of mammalian olfactory receptor neurons. *Journal of Membrane Biology* **161**, 163–171.

Hirst, G. D. S. & McLachlan, E. (1986). Development of dendritic calcium currents in ganglion cells of the rat lower lumbar sympathetic chain. *Journal of Physiology* **377**, 349–368.

Ireland, D. R., Davies, P. J. & McLachlan, E. M. (1998). The role of N-type Ca^{2+} channels in regulating excitability of guinea-pig sympathetic neurones. *Journal of the Autonomic Nervous System* **73**, 109–114.

Jaggar, J. H., Wellman, G. C., Heppner, T. J., Porter, V. A., Perez, G. J., Gollasch, M., Kleppisch, T., Rubart, M., Stevenson, A. S., Lederer, W. J., Knot, H. J., Bonev, A. D. & Nelson, M. T. (1998). Ca^{2+} channels, ryanodine receptors and Ca^{2+}-activated K^+ channels: a functional unit for regulating arterial tone. *Acta Physiologica Scandinavica* **164**, 577–587.

Jobling, P., McLachlan, E. M. & Sah, P. (1993). Calcium induced calcium release is involved in the afterhyperpolarization in one class of guinea pig sympathetic neurone. *Journal of the Autonomic Nervous System* **42**, 251–258.

Jones, S. W. & Jacobs, L. S. (1990). Dihydropyridine actions on calcium currents of frog sympathetic neurons. *Journal of Neuroscience* **10**, 2261–2267.

Kawai, T. & Watanabe, M. (1986). Blockade of Ca-activated K conductance by apamin in rat sympathetic neurones. *British Journal of Pharmacology* **87**, 225–232.

Kobayashi, M., Inoue, T., Matsuo, R., Masuda, Y., Hidaka, O., Kang, Y. N. & Morimoto, T. (1997). Role of calcium conductances on spike afterpotentials in rat trigeminal motoneurons. *Journal of Neurophysiology* **77**, 3273–3283.

McAfee, D. A. & Yarowsky, P. J. (1979). Calcium-dependent potentials in the mammalian sympathetic neurone. *Journal of Physiology* **290**, 507–523.

McLachlan, E. M., Davies, P. J., Häbler, H. J. & Jamieson, J. (1997). On-going and reflex synaptic events in rat superior cervical ganglion cells. *Journal of Physiology* **501**, 165–181.

Marrion, N. V. & Tavalin, S. J. (1998). Selective activation of Ca^{2+}-activated K^+ channels by co-localized Ca^{2+} channels in hippocampal neurons. *Nature* **395**, 900–905.

Martínez-Pinna, J., McLachlan, E. M. & Gallego, R. (1998). Different calcium sources for activation of chloride or potassium channels in sympathetic ganglion cells. *European Journal of Neuroscience* **10**, suppl. 10, 72.

Meissner, G. (1994). Ryanodine receptor/Ca^{2+} release channels and their regulation by endogenous effectors. *Annual Review of Physiology* **56**, 485–508.

Mintz, I. M., Adams, M. E. & Bean, B. P. (1992). P-type calcium channels in rat central and peripheral neurons. *Neuron* **9**, 85–95.

Namkung, Y., Smith, S. M., Lee, S. B., Skrypnyk, N. V., Kim, H.-L., Chin, H., Scheller, R. H., Tsien, R. W. & Shin, H.-S. (1998). Targeted disruption of the Ca^{2+} channel b_3 subunit reduces N- and L-type Ca^{2+} channel activity and alters the voltage-dependent activation of P/Q-type Ca^{2+} channels in neurons. *Proceedings of the National Academy of Sciences of the USA* **95**, 12010–12015.

Olivera, B. M., Miljanich, G. P., Ramachandran, J. & Adams, M. E. (1994). Calcium channel diversity and neurotransmitter release: the ω-conotoxins and ω-agatoxins. *Annual Review of Biochemistry* **63**, 823–867.

Osmanovic, S. S. & Shefner, S. A. (1993). Calcium-activated hyperpolarizations in rat locus coeruleus neurons *in vitro*. *Journal of Physiology* **469**, 89–109.

Randall, A. & Tsien, R. W. (1995). Pharmacological dissection of multiple types of Ca^{2+} channel currents in rat cerebellar granule neurons. *Journal of Neuroscience* **15**, 2995–3012.

Regan, L. J., Sah, D. W. Y. & Bean, B. P. (1991). Ca^{2+} channels in rat central and peripheral neurons: High-threshold current resistant to dihydropyridine blockers and omega-conotoxin. *Neuron* **6**, 269–280.

Robitaille, R., Garcia, M. L., Kaczorowski, G. J. & Charlton, M. P. (1993). Functional colocalization of calcium and calcium-gated potassium channels in control of transmitter release. *Neuron* **11**, 645–655.

Sacchi, O., Rossi, M. L. & Canella, R. (1995). The slow Ca^{2+}-activated K^+ current, I_{AHP}, in the rat sympathetic neurone. *Journal of Physiology* **483**, 15–27.

Sah, P. (1995). Different calcium channels are coupled to potassium channels with distinct electrophysiological roles in vagal neurons. *Proceedings of the Royal Society* B **260**, 105–111.

Sah, P. (1996). Ca^{2+}-activated K^+ currents in neurones: types, physiological roles and modulation. *Trends in Neurosciences* **19**, 150–154.

Sánchez-Vives, M. V. & Gallego, R. (1994). Calcium-dependent chloride current induced by axotomy in rat sympathetic neurons. *Journal of Physiology* **475**, 391–400.

Scott, R. H., McGuirk, S. M. & Dolphin, A. C. (1988). Modulation of divalent cation-activated chloride ion currents. *British Journal of Pharmacology* **94**, 653–662.

Shoshan-Barmatz, V. & Ashley, R. H. (1998). The structure, function and cellular regulation of ryanodine-sensitive Ca^{2+} release channels. *International Review of Cytology* **183**, 185.

Tanabe, M., Gähwiler, B. H. & Gerber, U. (1998). L-type Ca^{2+} channels mediate the slow Ca^{2+}-dependent afterhyperpolarization current in rat CA3 pyramidal cells in vitro. *Journal of Neurophysiology* **80**, 2268–2273.

Toth, P. T. & Miller, R. J. (1995). Calcium and sodium currents evoked by action potential waveforms in rat sympathetic neurones. *Journal of Physiology* **485**, 43–57.

Viana, F., Bayliss, D. A. & Berger, A. J. (1993). Multiple potassium conductances and their role in action potential repolarization and repetitive firing behavior of neonatal rat hypoglossal motoneurons. *Journal of Neurophysiology* **69**, 2150–2163.

Westenbroek, R. E., Hoskins, L. & Catterall, W. A. (1998). Localization of Ca^{2+} channel subtypes on rat spinal motor neurons, interneurons, and nerve terminals. *Journal of Neuroscience* **18**, 6319–6330.

Wikström, M. A. & El Manira, A. (1998). Calcium influx through N- and P/Q-type channels activate apamin-sensitive calcium-dependent potassium channels generating the late hyperpolarization in lamprey spinal neurons. *European Journal of Neuroscience* **10**, 1528–1532.

Acknowledgements

This work was supported by grants PM95-0107 and PM98-0102-C02-01 from the DGICYT of Spain and by grant 970852 from the National Health and Medical Research Council of Australia. J.M.-P. holds a graduate fellowship from the DGES of Spain. We thank Eva Quintero and Alfonso Pérez-Vegara for technical assistance and Félix Viana and James A. Brock for helpful comments on the manuscript.

Corresponding author

R. Gallego: Instituto de Neurociencias, Universidad Miguel Hernández-CSIC, Apartado 18, Campus de San Juan, 03550 San Juan de Alicante, Spain.

Email: roberto.gallego@umh.es